The impact of hot-melt extrusion on the tableting behaviour of polyvinyl alcohol

W. Grymonpré[1,*], W. De Jaeghere[1,*], E. Peeters[2], P. Adriaensens[3], J.P. Remon[1], C. Vervaet[1]

[1] Laboratory of Pharmaceutical Technology, Ghent University, Ghent, Belgium

[2] Laboratory of Pharmaceutical Process Analytical Technology, Ghent University, Ghent, Belgium

[3] Institute for Materials Research (IMO) – chemistry division, Hasselt University, Diepenbeek, Belgium

*Both authors equally contributed

Corresponding author:

C. Vervaet

Ghent University, Laboratory of Pharmaceutical Technology

Harelbekestraat 72

9000 Ghent (Belgium)

Tel.: +32 9 264 80 54

Fax: +32 9 222 82 36

E-mail address: Chris.Vervaet@UGent.be

Abstract

There is evidence that processing techniques like hot-melt extrusion (HME) could alter the mechanical properties of pharmaceuticals, which may impede further processability (e.g. tableting). The purpose of this study was to evaluate if HME has an impact on the tableting behavior of polyvinyl alcohol (PVA) – formulations. Mixtures of partially hydrolysed PVA grades (with a hydroxylation degree of 75 and 88%) and sorbitol (0, 10 and 40%) were extruded, (cryo-) milled and compressed into compacts of 350±10 mg. Before compression all intermediate products were characterized for their solid-state (T_g, T_m, crystallinity) and material properties (particle size, moisture content, moisture sorption). Because both PVA-grades required higher extrusion temperatures (>180 °C), sorbitol was added to PVA as plasticizing agent to allow extrusion at 140°C. Compaction experiments were performed on both physical mixtures and cryo-milled extrudates of PVA-sorbitol. By measuring tablet tensile strength and porosity in function of compaction pressure, tableting behavior was compared before and after HME by means of the CTC-profiles (compressibility, tabletability, compactibility). A higher amorphous content in the formulation (as a result of HME) negatively influenced the tableting behavior (i.e. lower tablet tensile strength). HME altered the mechanical properties towards more elastically deforming materials, thereby increasing tablet elastic recovery during decompression. The lower tensile strengths resulted from a combined effect of less interparticulate bonding areas (because of higher elastic recovery) and weaker bonding strengths per unit bonding area (between glassy particles).

Keywords: hot-melt extrusion, tableting, elastic recovery, polyvinyl alcohol, oral drug delivery, immediate release.

1. INTRODUCTION

Due to the application of high-throughput screening and medicinal chemistry as drug selection procedures, there has been a significant increase in the number of new chemical entities (NCE) that are poorly water-soluble. **Pharmaceutical research, shifted their focus to new formulation strategies, in order to overcome solubility-related problems, for which the formulation of solid dispersions was a viable technique to improve the (oral) bioavailability of poorly water-soluble drug compounds (Janssens and Van den Mooter, 2009; Leuner and Dressman, 2000).** Different approaches are reported in order to (molecularly) disperse the active pharmaceutical ingredient (API) in its carrier (Moneghini et al., 2001; Paudel et al., 2013; Sethia and Squillante, 2004), whereby hot-melt extrusion (HME) has the advantage of being a continuous manufacturing process that is generally applicable on industrial scale, without the requirement of further drying steps (Breitenbach, 2002).

Partially hydrolysed polyvinyl alcohols (PVA) were successfully screened as carriers in HME for immediate release applications, whereby PVA-grades with high degree of hydrolysis (70 – 90%) were most promising, as drug release was independent of pH (1-9) and ionic strength (0 – 0.14M) (De Jaeghere et al., 2015). However, PVA-grades with high degree of hydrolysis (> 70%) have a rather high melting point onset (150-170°C), indicating that higher extrusion temperatures are needed in order to extrude these polymers, which impedes the use of thermosensitive API. De Jaeghere et al. evaluated sorbitol as plasticizer for PVA and noticed a sufficient decrease in process temperature, which could extend the application of PVA as carrier in HME (De Jaeghere et al., 2015).

Various downstream processes for HME are available, from injection molding (i.e. finale dosage form) to milling of the extrudates (i.e. intermediate products) for further processability (e.g. tablets) (Treffer et al., 2013). Tablets are still the most popular dosage forms for the pharmaceutical industry and patient since they allow high-precision dosing, ensure patient compliance and provide high manufacturing efficiency. **Therefore, previous**

research was extended to investigate the processability of PVA and PVA-sorbitol carriers after HME into conventional tablets. The impact of solid dispersion manufacturing techniques such as HME on the tableting behaviour of pharmaceutical polymers whether or not with plasticizer, was only limited investigated (Agrawal et al., 2013; Boersen et al., 2013; Dinunzio et al., 2012; Mohammed et al., 2012) with minimal focus on the mechanical properties of the pure components. These properties are of great importance in solid dosage form development and manufacturing, as they describe the behaviour of a material subjected to an applied stress **(Iyer et al., 2013). In this study, PVA and physical mixtures of PVA-sorbitol were processed by HME, characterized, milled to powders of appropriate particle size and eventually processed into tablets.** CTC-profiles (compressibility, tabletability, compactibility) of those tablets were drafted and compared with the physical mixtures in order to evaluate the impact of different processing steps on the mechanical properties of these materials. Axial recoveries of the tablets were calculated and linked to the CTC-profiles.

2. MATERIALS AND METHODS

2.1. Materials

Two types of polyvinyl alcohol (PVA) were used, a technical grade PVA_{505} (72-75 % hydrolysed) obtained from Kuraray (Hattersheim am Main, Germany) and a pharmaceutical grade $PVA_{4\text{-}88}$ (88% hydrolysed) obtained from Merck (Darmstadt, Germany). Sorbitol (Fagron, Waregem, Belgium) was used as water-soluble plasticizer and celecoxib (CEL) (Sanico, Turnhout, Belgium) was used as model drug.

2.2. Hot-Melt Extrusion (HME)

Physical mixtures of PVA and sorbitol (0, 10, 40 %) were processed with a co-rotating, fully intermeshing twin-screw extruder (Prism Eurolab 16, Thermo Fisher, Germany) operating at a screw-speed of 100 rpm and **a process temperature of 180 °C across the entire barrel**. The extruder was equipped **with a gravimetric feeder (0.300 kg/h**), two co-rotating twin-screws with 3 mixing zones and a cylindrical die of 3 mm. The extrudates were quench-cooled with liquid nitrogen, (cryo)-milled and sieved through a 300-micron sieve **(De Jaeghere et al., 2015)**.

2.3. Tableting

Tablets (350 ± 10 mg) of physical mixtures and cryo-milled extrudates of PVA-sorbitol were prepared using a rotary tablet press (MODUL™ P, GEA Pharma Systems, Courtoy™, Halle, Belgium) equipped with a round concave (radius: 24mm) Euro B punch of 12 mm diameter at a tableting speed of 5 rpm. The compaction pressure ranged from 100 to 400 MPa after a pre-compression at 17 MPa. Tablets used for thermal analysis were compacted at 305 MPa, after pre-compression at 17 MPa. All tablets were immediately after compression characterized for tablet strength, dimensions and mass.

2.4. Characterization

2.4.1. Thermal analysis

Differential scanning calorimetry (DSC) was performed before and after sample manipulation (HME, cryo-milling, tableting), whereby melting temperature (T_m), glass transition temperature (T_g), crystallization temperature (T_c) and heat of fusion (ΔH_f) was analysed with a Q2000 DSC (TA Instruments, Leatherhead, UK) equipped with a refrigerated cooling system (RCS). The DSC cell was purged with dry nitrogen at a flow rate of 50 ml/min. The samples were evaluated according to DSC conditions (heating rate of 10 °C/min) during 3 cycles (heating, cooling and heating) from -20 to 200 °C. Crystallinity (%) was calculated with reference to the enthalpy of fusion (ΔH_f^*) of a perfect PVA crystal (138.6 J/g) (Mallapragada et al., 1997) with the following formula:

$$X_c = \left(\frac{\Delta Hf}{\Delta Hf*}\right) x\ 100$$

All results were analysed in **triplicate** using the TA instrument Universal Analysis 2000 software. **A one-way analysis of variance (ANOVA) was performed with SPSS Statistics 23 (IBM, New York, United States) to detect significant differences in T_g or T_m during extrusion, cryomilling and tableting of both PVA-grades. Tukey analysis was used to determine differences in T_g and T_m between extrusion, cryomilling and tableting.**

2.4.2. X-ray diffraction

The crystallinity of PVA, sorbitol and CEL was investigated by means of X-ray diffraction. The X-ray diffraction patterns were determined using a D5000 Cu Kα diffractor (λ = 0.154 nm) (Siemens, Karlsruhe, Germany) with a voltage of 40 V in the angular range of $10^\circ < 2\theta < 60°$ using a step scan mode (step width = 0.02°, counting time = 1s/step).

2.4.3. Solid-state ^{1}H-NMR

Solid-state ^{1}H-wideline NMR measurements were carried out at ambient temperature on a Varian Inova 400 spectrometer in a dedicated wide-line probe equipped with a 5 mm coil using

the solid echo method (Mens et al., 2008). The samples were placed in 5 mm glass tubes, which were closed tightly with Teflon stoppers.

The T_{1H} relaxation decay times (spin-lattice relaxation in the lab frame) were measured by placing an inversion recovery filter in front of the solid echo part ($180°_{x'}$ - t - $90°_{x'}$ - t_{se} - $90°_{y'}$ - t_{se} - acquire). The length of the 90° pulse (t_{90}) was set to 1.6 µs and spectra were recorded with a spectral width of 2 MHz (0.5 µs dwell time), allowing an accurate determination of the echo maximum which is formed at $\tau = (3t_{90}/2 + 2t_{se}) = 7$ µs and this time point is calibrated to time zero. The integrated proton signal intensity was analyzed mono- or bi-exponentially as a function of the variable inversion time t according to:

$$I(t) = I_0^S \left(1 - 2\exp\left(-{}^{t}/_{T_{1H^S}}\right)\right) + I_0^L \left(1 - 2\exp\left(-{}^{t}/_{T_{1H^L}}\right)\right) + C^{ste}$$

'S' and 'L' refer to the fractions with short and long decay time, respectively.

All experimental data were analyzed using a non-linear least-squares fit (Levenberg-Marquardt algorithm). A preparation delay of 5 times the longest T_{1H} relaxation decay time was always respected between successive accumulations to obtain quantitative results.

2.4.4. Particle size distribution

Particle size distribution (PSD) of the powders was measured by laser diffraction (Mastersizer-S long bench, Malvern Instruments, Malvern, UK). The measurements were done via dry dispersion method in volumetrical distribution mode using a 300 RF lens combined with a dry powder feeder (Malvern Instruments, Malvern, UK) at a feeding rate of 3.0 G and a jet pressure of 2.0 Bar. Measurements were performed in **triplicate**.

2.4.5. Dynamic vapour sorption

Dynamic vapour sorption (DVS Advantage, Surface Measurement Systems, Middlesex, UK) was used to assess the overall hygroscopicity of the materials. Approximately 10-20 mg of sample was placed into the instrument microbalance where it was dried under a stream of dry nitrogen at 25°C until equilibrium (i.e. a weight change of less than 0.002 % per minute during at least 15 min). The samples were subsequently exposed to various relative humidities (RH)

171 at 25°C, increasing from 0 to 80 % in steps of 20 %, from 80 to 90 % and from 90 to 98 %
172 allowing equilibration at each interval.

173 **2.5. Tablet Evaluation**

174 **Tablet evaluations were performed onto ten tablets.**

175

176 *2.5.1. Tensile strength, breaking force and dimensions*

177 Tablet breaking force, diameter and thickness were determined using a hardness tester (Type
178 HT10, Sotax, Basel, Switzerland). Tablet diametral tensile strength of the tablets (MPa) was
179 derived using the following equation of Fell and Newton (1968):

180 $$\textit{Tablet Tensile Strength } (\sigma_t) = \frac{2P}{\pi D t}$$

181 where P, D and t denote the diametral breaking force (N), tablet diameter (mm) and tablet
182 thickness (mm), respectively. This formula can be used for double-convex cylindrical tablets
183 as was reported by Podczeck et al. (Podczeck et al., 2013).

184 *2.5.2. Tablet porosity*

185 The porosity of the formed compacts was calculated using the following equation:

186 $$\textit{Tablet Porosity} = 1 - \frac{\rho_{app}}{\rho_{true}}$$

187 where ρ_{app} and ρ_{true} denote the apparent and true density (g/ml), respectively. Apparent
188 density was calculated by dividing the tablet mass by the volume of the tablet, while the true
189 density of all powders was measured using helium pycnometry (AccuPyc 1330, Micrometrics,
190 Norcross, U.S.A) at an equilibration rate of 0.0050 psig/min with the number of purges set to
191 10.

192 *2.5.3 Tablet compaction characterization*

193 Compacts were prepared at different compaction pressures (100 to 400 MPa with a pre-
194 compression of 17 MPa), and tableting behaviour (tabletability, compressibility and
195 compactibility) was evaluated.

196 *Tabletability* was analysed by plotting tablet tensile strength to the compaction pressure.
197 *Compressibility* was analysed by assessment of the tablet volume reduction (tablet porosity
198 normalised by compaction pressure). *Compactibility* of pharmaceutical powders is generally
199 described by use of the Ryshkewitch equation:

200 $$\sigma_t = \sigma_0 \, e^{-bP}$$

201 where σ_t and σ_0 denotes the tablet tensile strength (MPa) and limiting tablet tensile strength
202 at zero porosity (MPa), respectively, b is an empirical constant and P denotes the tablet
203 porosity (Ryshkewitch, 1953).

204 *2.5.4. Axial recovery*

205 Axial recovery of the tablets immediately after ejection (IAR) was calculated by use of the
206 Armstrong and Haines-Nutt equation (Armstrong and Haines-Nutt, 1972):

207 $$IAR\ (\%) = \left(\frac{T_a - T_{id}}{T_{id}}\right) x100$$

208 where T_a denotes the tablet height immediately after ejection (mm) and T_{id} the tablet height
209 under maximum compression force at main compression (mm). The dimensions of 10 tablets,
210 manufactured at equal conditions, were used to calculate the % IAR of each formulation at 4
211 compaction pressures.

3. RESULTS AND DISCUSSION

3.1. Characterization

Thermal stability of PVA_{505} and $PVA_{4\text{-}88}$ was evaluated by means of thermogravimetric analysis (TGA) (data not shown). This technique showed an onset of thermal polymer degradation at 240°C, which indicated that PVA polymers are stable under the process conditions used in this study (maximum extrusion temperature of 180°C was used) (Alexy et al., 2004; De Jaeghere et al., 2015; Peng and Kong, 2007).

Previous research work already showed the ability of sorbitol to act as low molecular weight plasticizer of PVA. Therefore, melting of PVA-sorbitol mixtures was required to establish molecular interactions between polymer and sorbitol, as no effect of sorbitol was observed during 1st DSC heating cycle. The plasticizing effect of sorbitol was linked to its concentration as more interactions can be established between the OH-groups of both components, thus disrupting the structural regularity of PVA (De Jaeghere et al., 2015). DSC analysis was used to examine the influence of extrusion, cryo-milling and tableting on the physicochemical properties of PVA and sorbitol. T_g of sorbitol was lower in the cryo-milled extrudates due to their higher water content (an increase of 1-1.5% was observed compared to HME samples): after HME and cryo-milling T_g was -8.1±0.3°C and -15.5±0.1°C, respectively, for PVA_{505} and -3.6±0.2°C and -14.5±1.6°C, respectively, for $PVA_{4\text{-}88}$. **ANOVA showed no significant difference ($p > 0.05$) in T_g of both PVA-grades during extrusion, cryo-milling and tableting, however significant difference ($p < 0.05$) was observed in T_m of both PVA-grades, which was slightly increased during processing (Table 1).**

DSC analysis showed endothermic peaks between 60-75°C and after 1 week X-ray diffraction patterns showed some degree of crystallinity in the samples (Fig.1). This phenomena was linked to the crystallization of sorbitol polymorphs during storage (Nezzal et al., 2009; Sztatisz et al., 1977). Due to this (re)-crystallization of sorbitol, the plasticizing effect of sorbitol was reduced and T_m of PVA slightly increased. Furthermore, solid-state ^{1}H-wideline NMR (Table 2)

was performed, whereby a short relaxation decay time of 6.3s was found for semi-crystalline PVA_{4-88}, and a long relaxation decay time of 26.3s for crystalline sorbitol. After extrusion, PVA_{4-88} and sorbitol interacted with each other, as both fractions (I_0^S and I_0^L) were changed compared to the physical mixtures and the relaxation decay times of PVA_{4-88} and sorbitol were decreased. However, phase separation was observed for extrudates containing 40% sorbitol, as evidenced by the presence of 2 relaxation decay times. Therefore, experiments were repeated with extrudates containing less sorbitol (i.e. 10%), whereby only one relaxation decay time of 14.2s was observed, which could mean that sorbitol was homogenized with PVA_{4-88} and more stable inside the extrudates. This result was linked to the DSC results whereas no re-crystallization of sorbitol was observed.

PSD of both PVA-grades and sorbitol were measured by means of laser diffraction (Table 3). Although all powders were sieved to a fraction smaller than 300 micron, d_{90} –values exceeded 300 micron for all samples as there was a tendency for the material to agglomerate during the measurements. Fine powders are more subjected to agglomeration since their small particle size increases surface-mass ratio, which favours the bonding (Parikh, 2010).

DVS was used to calculate moisture sorption and desorption isotherms in order to assess the hygroscopic behavior of the PVA-sorbitol mixtures (physical mixtures and cryo-milled extrudates) (Fig.2). The influence of sorbitol was clearly visible at extreme conditions (21°C/98%RH) as non-extruded PVA (A) had a water content of 30 %, which increased up to 80% by addition of sorbitol (C). This was expected from the sorption isotherms of crystalline sorbitol (data not shown) which revealed water contents >80% at equal conditions. The level of hysteresis was negligible for pure PVA before and after extrusion (A,B) which could be attributed to intermolecular hydrogen bondings between the polymer chains (Assender and Windle, 1998), whereby the hydroxyl groups of PVA are not available for binding with water molecules. Interestingly, when comparing PVA-sorbitol (60:40) before and after extrusion (C,D) there was a remarkable difference in the level of hysteresis. While for the non-extruded formulation hysteresis was clearly present, it became negligible for the extruded formulation.

This was explained by DSC data which showed that interactions between PVA and sorbitol only occurred when sorbitol was melted by HME (De Jaeghere et al., 2015). The resulting extrudates are dense particles (Page and Maurer, 2014). It has been described in literature that for amorphous sugars the packing of molecules affected the water sorption behaviour. In dense glassy particles, adsorption of water occurs mainly on the surfaces (weak interactions) because of the absence of pores penetrable to water (Jouppila, 2006).

This is applicable for the PVA-sorbitol extrudates, since DSC results revealed that amorphous sorbitol clusters are present in the PVA carrier (separate T_g for sorbitol and PVA). The moisture content of all formulations was lower (< 5 %) at laboratory conditions (35-60 % RH).

3.2. Tablet properties

3.2.1. Tabletability

Tabletability describes the relationship between tensile strength of a tablet and compaction pressure exerted on these tablets (Fig.3) (Joiris et al., 1998). A strong increase of tablet strength was observed at low compaction pressures for most mixtures, however the curves leveled off at higher compaction pressures. This was explained by the phenomenon of elastic recovery, which occurred after removal of the compaction load (i.e. decompression).

As powders are compressed, particles come in closer contact by volume reduction mechanisms (particle rearrangements, fragmentation, plastic/elastic deformation), which reduced tablet porosity. This leads to a steep increase in the bonding area and consequently in tensile strength of the tablets (Duberg and Nyström, 1986). In the low-pressure region, elastic recovery of the tablet after compression was negligible and the tablet strength increased linear with the compaction pressure. At higher compaction pressures, tablet porosity was already reduced considerably so further increase of the compaction pressure led to elastic deformation rather than a further decrease in porosity (Sun and Grant, 2001). Inevitable, such particles store elastic energy, which is linked to a certain elastic recovery at decompression, thereby reducing the bonding area. The associated reduced points of contact between

291 neighbouring particles in the tablet caused a level off in tensile strength (Sun, 2011). In general,
292 tabletability curves of the extrudates were lower than those of the physical mixtures and the
293 increase in tablet strength was limited (i.e. level off at lower compaction pressures). These
294 results were in line with earlier findings on the tabletability of HME materials (Agrawal et al.,
295 2013; Boersen et al., 2013). While the tensile strength of physical mixtures increased in
296 function of the concentration of crystalline sorbitol (a value of 2.5 MPa was recorded for 40 %
297 sorbitol at a compaction pressure of 300 MPa), the tensile strength of extruded samples was
298 lower at higher amorphous sorbitol content (at 40 % sorbitol content the tablets manufactured
299 at various compaction pressures were even too soft for measuring the diametrical breaking
300 force) (Fig. 3, A). In addition, maximum tabletability (i.e. highest tensile strength) was obtained
301 at lower compaction pressures for extrudates compared to physical mixtures, at about 200
302 MPa and > 400 MPa, respectively (Fig.3, B). Differences in particle size (Table 2) could explain
303 the lower position of the curves but could not explain the limited increase in tablet strength and
304 the early level off at lower compaction pressures. Agrawal et al. attributed this to the possible
305 weaker interactions between glassy materials resulting in tablets with lower tensile strengths
306 (Agrawal et al., 2013). In this study it was hypothesized that the process of HME altered the
307 mechanical properties of the PVA-sorbitol-carrier and therefore changed its volume reduction
308 mechanism towards a more elastically deforming material. Iyer et al. reported an increase in
309 the elasticity of melt-extruded HPMC-AS and linked this with a likely higher elastic recovery
310 after compression (Iyer et al., 2013). It is possible that the HME-process induced a similar
311 change in the elastic deformation of PVA-sorbitol, leading to higher elastic recoveries with
312 increasing amorphous fraction (Fig.1: the absence of sharp crystalline peaks in the XRD-data
313 of cryo-milled extrudates compared to the physical mixtures). Boersen et al. reported similar
314 findings, where brittle fracture index experiments showed a reduction in the plasticity of HME-
315 powders (Boersen et al., 2013).

316 Comparison of figures A and B indicated that physical mixtures of non-extruded $PVA_{4\text{-}88}$ yielded
317 tablets of higher tensile strengths than physical mixtures of PVA_{505} at equal compaction

pressures (an increase of 80 % in tensile strength was recorded at a compaction pressure of 300 MPa). This was explained by the differences in crystalline content of both polymers, since PVA is a semi-crystalline polymer (Agrawal et al., 2013). The crystalline content of pure PVA_{4-88} (32.1%) was significantly higher compared to pure PVA_{505} (16.6%), which resulted in 'stronger' tablets, and HME reduced the crystallinity of PVA_{4-88} significantly (21.4%) compared to PVA_{505} (14.4%) as the higher extrusion temperatures disrupted inter- and intramolecular hydrogen bonding. Additionally, differences in PSD of the physical mixtures (Table 2) also contributed to this phenomenon.

Tabletability on its own does not provide a fundamental understanding of the tableting behaviour of pharmaceutical powders, since bonding area (reflected by compressibility) and bonding strength per unit bonding area (reflected by compactibility) also determine the tensile strength of tablets. Only by simultaneously analysing particle size, compressibility, compactibility and tabletability, an extensive insight in the tablet properties can be obtained (Sun and Grant, 2001).

3.2.2. Compressibility

Compressibility of a material is its ability to be reduced in volume as a result of an applied pressure (Joiris et al., 1998). The compressibility profiles showed similar trends as tabletability, with physical mixtures having greater compressibility (i.e. yielding lower tablet porosities) compared to the extrudates (Fig. 4). While the lowest tablet porosities were observed for physical mixtures with higher content of crystalline sorbitol, porosities increased in extrudates with more amorphous content (i.e. high sorbitol content). In addition, maximum compressibility (i.e. lowest tablet porosity) was obtained at a lower compaction pressures for extrudates containing (amorphous) sorbitol compared to physical mixtures, at about 250 MPa and >400 MPa, respectively (Fig. 4). The differences between physical mixtures and extrudates were linked to HME. A higher amorphous content in the extrudates induced an early level off in the compressibility profiles, resulting in constant tablet porosity at higher compaction pressures because of the effect of elastic recovery (Fig. 4). These results were in line with tabletability

345 profiles where an early flattening was observed in tablet tensile strength of the extrudates.
346 Therefore, the assumption of a altered volume reduction mechanism due to hot-melt extrusion
347 was strengthened. If HME altered the mechanical properties of PVA-sorbitol towards a more
348 elastical deforming material, the stored elastic energy increased in function of the applied
349 external force and hence resulted in more elastic recovery of the tablets during decompression
350 (Sun and Grant, 2001). Therefore, the reduced porosity due elastic deformation was
351 counteracted by the elastic recovery causing a level off in the curve.

352 By comparing tablet porosities at equal compaction pressures for physical mixtures of PVA_{505}
353 and $PVA_{4\text{-}88}$, it was clear that particle size had a strong influence. Lower tablet porosities were
354 detected with $PVA_{4\text{-}88}$ –mixtures (tablet porosity was 0.14 and 0.08 for physical mixtures with
355 $PVA_{4\text{-}88}$ and PVA_{505}, respectively), since these had smaller particle sizes (Table 2). However,
356 the effect of extrusion on the pure polymers was clearly visible. While for PVA_{505} the curves of
357 physical mixtures and extrudates are superimposed (Fig.4,A), this is not the case for $PVA_{4\text{-}88}$
358 since higher tablet porosities were reached for the extrudates of $PVA_{4\text{-}88}$ (Fig.4,B). This was
359 explained by the differences in crystalline content of both polymers. Extrusion of pure $PVA_{4\text{-}88}$
360 increased the amorphous fraction of the semi-crystalline polymer, which favoured elastic
361 deformation and hence increased the elastic recovery. This was not the case for pure PVA_{505},
362 since the crystalline content did not changed remarkably.

363 3.2.3. Compactibility

364 Compactibility describes the relationship between tensile strength and porosity (Fig.5). Tablet
365 tensile strength decreased exponentially with increasing porosities, as described by the
366 Ryshkewitch equation (Ryshkewitch, 1953). Although physical mixtures and extrudates
367 showed large differences in tabletability (i.e. tensile strengths), these differences were less
368 distinct when tablet tensile strength was plotted at zero porosity, especially for PVA_{505}.

369 Since compactibility can be used to quantify bonding strength between particles at zero
370 porosity (Joiris et al., 1998; Maarschalk et al., 1996; Sun, 2011), these results suggested that

371 the higher tensile strength was more related to the interparticulate bonding area (i.e.
372 compressibility) compared to the bonding strength per unit bonding area (i.e. compactibility).
373 However, compactibility curves of both PVA-types gave evidence of weaker interactions
374 between glassy materials (Agrawal et al., 2013) since compression of physical mixtures with
375 increasing sorbitol content (i.e. higher crystalline fraction) resulted in a higher tensile strength
376 at zero porosities. This effect was clearly reflected in the lower position of the compactibility
377 curve of pure $PVA_{4\text{-}88}$ extrudates compared to the physical mixture (Fig.5, B), which was linked
378 to the lower crystalline content of the semi-crystalline polymer after HME. This effect was not
379 significant for PVA_{505} and therefore those curves (PM vs. EX) were almost superimposed at
380 zero porosity (Fig.5,A), indicating that almost no changes in bonding strength occurred. In
381 general, this study revealed that differences in tablet tensile strength for PVA-sorbitol carriers
382 were the result of altered interparticulate bonding areas (elastic recovery and particle size)
383 combined with a change in the bonding strengths for glassy materials (Agrawal et al., 2013)
384 after extrusion.

385 3.2.4. Axial recovery

386 Axial recovery of the tablets calculated immediately after tablet ejection (IAR) was selected as
387 the “out-of-die” recovery descriptor. For each formulation, IAR was calculated for tablets of
388 non-extruded physical mixtures and extruded mixtures at 4 compaction pressures. The results
389 are shown in Fig.6 as a ratio of the IAR before and after extrusion in function of the compaction
390 pressure.

391 All calculated ratios were higher or equal to the value 1 indicating that tablets of extruded
392 powders experienced higher or equal IAR compared to tablets of their physical mixtures (i.e.
393 not subjected to HME). Only for pure PVA_{505}, HME had no impact on the IAR-ratio of the tablets
394 (ratio = 1), as no change in crystalline content of pure PVA_{505}-polymer was observed after HME.
395 However, IAR-ratios of pure $PVA_{4\text{-}88}$ were > 1 since HME affected the amorphous content of
396 the polymer. The addition of sorbitol to the formulations, which changed from crystalline to
397 amorphous state after HME, resulted in higher %IAR ratios of the tablets. These results

showed that the higher amorphous content of formulations due to HME was reflected in the IAR of the tablets. Additionally, these results were in line with the CTC-profiles and confirmed the hypothesis that due to HME, materials were transformed towards a more amorphous state, hereby experiencing more elastic deformation during compression.

4. CONCLUSIONS

This study demonstrated that HME could alter the mechanical properties of PVA-sorbitol carriers, thereby negatively affecting the tableting behaviour (i.e. lowering tablet tensile strength) with increasing amorphous content. This resulted from a combined effect of less interparticulate bonding areas (because of higher elastic recoveries) and weaker bonding strengths per unit bonding area (i.e. lower tensile strengths at zero porosity). In general, it can be concluded that it will be necessary to further optimize the formulation (e.g. plasticizer content) in order to improve the tableting behaviour of PVA-sorbitol extrudates.

410 **Acknowledgements**

411 The authors acknowledge the support of Merck for providing the pharmaceutical grade PVA
412 samples ($PVA_{4\text{-}88}$) and Kuraray for providing the technical grade PVA samples (PVA_{505}).

5. LITERATURE

Agrawal, A.M., Dudhedia, M.S., Patel, A.D., Raikes, M.S., 2013. Characterization and performance assessment of solid dispersions prepared by hot melt extrusion and spray drying process. Int. J. Pharm. 457, 71–81. doi:10.1016/j.ijpharm.2013.08.081

Alexy, P., Lacik, I., Simkova, B., Bakos, D., Pronayova, N., Liptaj, T., Hanzelova, S., Varosova, M., 2004. Effect of melt processing on thermo-mechanical degradation of poly (vinyl alcohol) s. Polym. 85, 823–830. doi:10.1016/j.polymdegradstab.2004.02.011

Armstrong, N.A., Haines-Nutt, R.F., 1972. Elastic recovery and surface area changes in compacted powder systems. J. Pharm. Pharmacol. 24, Suppl:135P–136. doi:10.1016/0032-5910(74)80054-9

Assender, H.E., Windle, A.H., 1998. Crystallinity in poly(vinyl alcohol). 1. An X-ray diffraction study of atactic PVOH. Polymer (Guildf). 39, 4295–4302. doi:10.1016/S0032-3861(97)10296-8

Boersen, N., Lee, T.W.-Y., Shen, X.G., Hui, H.-W., 2013. A preliminary assessment of the impact of hot-melt extrusion on the physico-mechanical properties of a tablet. Drug Dev. Ind. Pharm. 9045, 1–9. doi:10.3109/03639045.2013.828216

Breitenbach, J., 2002. Melt extrusion : from process to drug delivery technology. Eur. J. Pharm. Biopharm. 54, 107–117.

De Jaeghere, W., De Beer, T., Van Bocxlaer, J., Remon, J.P., Vervaet, C., 2015. Hot-melt extrusion of polyvinyl alcohol for oral immediate release applications. Int. J. Pharm. 492, 1–9. doi:10.1016/j.ijpharm.2015.07.009

Dinunzio, J.C., Schilling, S.U., Coney, A.W., Hughey, J.R., Kaneko, N., Mcginity, J.W., 2012. Use of highly compressible Ceolus ™ microcrystalline cellulose for improved dosage form properties containing a hydrophilic solid dispersion. Drug Dev. Ind. Pharm. 38, 180–189. doi:10.3109/03639045.2011.595415

Duberg, M., Nyström, C., 1986. Studies on direct compression of tablets XVII. Porosity—pressure curves for the characterization of volume reduction mechanisms in powder compression. Powder Technol. 46, 67–75. doi:10.1016/0032-5910(86)80100-0

Iyer, R., Hegde, S., Zhang, Y.E., Dinunzio, J., Singhal, D., Malick, a., Amidon, G., 2013. The impact of hot melt extrusion and spray drying on mechanical properties and tableting indices of materials used in pharmaceutical development. J. Pharm. Sci. 102, 3604–3613. doi:10.1002/jps.23661

Janssens, S., Van den Mooter, G., 2009. Review: physical chemistry of solid dispersions. J. Pharm. Pharmacol. 61, 1571–1586. doi:10.1211/jpp/61.12.0001

Joiris, E., Martino, P. Di, Berneron, C., Guyot-Hermann, A.-M., Guyot, J.-C., Joiris, J.-C., 1998. Compression Behavior of Orthorhombic Paracetamol. Pharm. Res. 15, 1122–1130. doi:10.1023/A:1011954800246

Jouppila, K., 2006. Mono- and Disaccharides: Selected Physicochemical and Functional Aspects, in: Eliasson, A.-C. (Ed.), Carbohydrates in Food. Taylor&Francis Group, pp. 41–88.

Leuner, C., Dressman, J., 2000. Improving drug solubility for oral delivery using solid dispersions. Eur. J. Pharm. Biopharm. 50, 47–60. doi:10.1016/S0939-6411(00)00076-X

Maarschalk, K.V.D.V., Zuurman, K., Vromans, H., Bolhuis, G.K., 1996. Porosity expansion of tablets as a result of bonding and deformation of particulate solids. Int. J. Pharm. 140, 185–193. doi:10.1016/0378-5173(96)04584-X

Mallapragada, S.K., Peppas, N. a., Colombo, P., 1997. Crystal dissolution-controlled release systems. II. Metronidazole release from semicrystalline poly(vinyl alcohol) systems. J. Biomed. Mater. Res. 36, 125–130. doi:10.1002/(SICI)1097-4636(199707)36:1<125::AID-JBM15>3.0.CO;2-H

Mohammed, N.N., Majumdar, S., Singh, A., Deng, W., Murthy, N.S., Pinto, E., Tewari, D., Durig, T., Repka, M.A., 2012. Klucel ™ EF and ELF polymers for immediate-release oral dosage forms prepared by melt extrusion technology 13, 1158–1169. doi:10.1208/s12249-012-9834-z

Moneghini, M., Kikic, I., Voinovich, D., Perissutti, B., Filipović-Grcić, J., 2001. Processing of carbamazepine-PEG 4000 solid dispersions with supercritical carbon dioxide: preparation, characterisation, and in vitro dissolution. Int. J. Pharm. 222, 129–138. doi:10.1016/S0378-5173(01)00711-6

Nezzal, A., Aerts, L., Verspaille, M., Henderickx, G., Redl, A., 2009. Polymorphism of sorbitol. J. Cryst. Growth 311, 3863–3870. doi:10.1016/j.jcrysgro.2009.06.003

Page, S., Maurer, R., 2014. Downstream Processing Considerations, in: Shah, N., Sandhu, H., Choi, D.S., Chokshi, H., Malick, A.W. (Eds.), Amorphous Solid Dispersions: Theory and Practice. Springer, pp. 395–417.

Parikh, D.M., 2010. Introduction, in: Parikh, D.M. (Ed.), Pharmaceutical Handbook of Granulation Technology. Informa healthcare, pp. 2–3.

Paudel, A., Worku, Z.A., Meeus, J., Guns, S., Van Den Mooter, G., 2013. Manufacturing of solid dispersions of poorly water soluble drugs by spray drying: Formulation and process considerations. Int. J. Pharm. 453, 253–284. doi:10.1016/j.ijpharm.2012.07.015

Peng, Z., Kong, L.X., 2007. A thermal degradation mechanism of polyvinyl alcohol / silica nanocomposites. Polym. Degrad. Stab. 92, 1061–1071. doi:10.1016/j.polymdegradstab.2007.02.012

Podczeck, F., Drake, K.R., Newton, J.M., 2013. Investigations into the tensile failure of doubly-convex cylindrical tablets under diametral loading using finite element methodology. Int. J. Pharm. 454, 412–424. doi:10.1016/j.ijpharm.2013.06.069

Ryshkewitch, E., 1953. Compression Strength of Porous Sintered Alumina and Zirconia. J. Am. Ceram. Soc. 36, 65–68. doi:10.1111/j.1151-2916.1953.tb12837.x

Sethia, S., Squillante, E., 2004. Solid dispersion of carbamazepine in PVP K30 by conventional solvent evaporation and supercritical methods. Int. J. Pharm. 272, 1–10. doi:10.1016/j.ijpharm.2003.11.025

Sun, C., Grant, D.J.W., 2001. Influence of crystal structure on the tableting properties of sulfamerazine polySun, C., & Grant, D. J. W. (2001). Influence of crystal structure on the tableting properties of sulfamerazine polymorphs. Pharmaceutical Research, 18(3), 274–280. doi:10.1023. Pharm. Res. 18, 274–280. doi:10.1023/A:1011038526805

Sun, C.C., 2011. Decoding Powder Tabletability: Roles of Particle Adhesion and Plasticity. J. Adhes. Sci. Technol. 25, 483–499. doi:10.1163/016942410X525678

Sztatisz, J., Gál, S., Fodor, L., Pungor, E., 1977. Thermal investigations on the crystallization of sorbitol. J. Therm. Anal. 12, 351–360. doi:10.1007/BF01909593

Treffer, D., Wahl, P., Markl, D., Koscher, G., Roblegg, E., Khinast, J.G., 2013. Hot Melt Extrusion as a Continuous Pharmaceutical Manufacturing Process, in: Repka, M.A., Langley, N., Dinunzio, J. (Eds.), Melt Extrusion: Materials, Technology and Drug Product Design. Springer, pp. 363–396. doi:10.1007/978-1-4614-8432-5

Figure 1: XRD profiles (left) of sorbitol (A), physical mixture PVA-sorbitol (60:40**)** (B), cryom. extrudate (C) and cryom. extrudate after 1 week (D). DSC profiles (right) of extrudate (EX) and cryom. extrudate after at time point 0 and after 1 week.

Figure 2: DVS sorption (_) and desorption (…) curves of $PVA_{4\text{-}88}$ (A) , $PVA_{4\text{-}88}$ cryomilled extrudate (B), $PVA_{4\text{-}88}$-sorbitol (60:40) physical mixture (C), $PVA_{4\text{-}88}$-sorbitol (60:40) cryomilled extrudate (D) and sorbitol (E) at 21 °C.

Figure 3: Tabletability of physical mixtures (PM) and hot-melt extruded (EX) samples formulated with PVA_{505} (A) or $PVA_{4\text{-}88}$ (B),, in combination with 0, 10 or 40% sorbitol **(n=10).**

Figure 4: Compressibility of physical mixtures (PM) and hot-melt extruded (EX) samples formulated with PVA_{505} (A) and $PVA_{4\text{-}88}$ (B), in combination with 0, 10 or 40% sorbitol **(n=10).**

Figure 5: Compactibility of physical mixtures (PM) and hot-melt extruded (EX) samples formulated with PVA_{505} (A) or $PVA_{4\text{-}88}$ (B), in combination with 0, 10 or 40% sorbitol **(n=10).**

Figure 6: IAR-ratio of physical mixtures (PM) and hot-melt extruded samples (EX) at various compaction pressures for formulations containing PVA and sorbitol **(n=10)**.

Figure 1: XRD profiles (left) of sorbitol (A), physical mixture PVA-sorbitol (60:40**)** (B), cryom. extrudate (C) and cryom. extrudate after 1 week (D). DSC profiles (right) of extrudate (EX) and cryom. extrudate after at time point 0 and after 1 week.

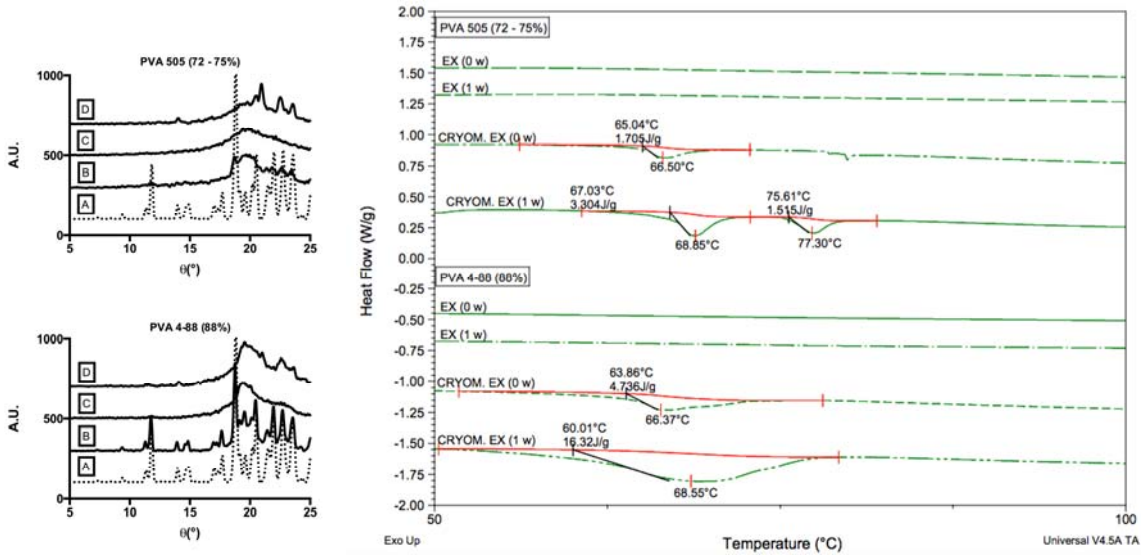

527 Figure 2: DVS sorption (_) and desorption (…) curves of $PVA_{4\text{-}88}$ (A) , $PVA_{4\text{-}88}$ cryomilled
528 extrudate (B), $PVA_{4\text{-}88}$-sorbitol (60:40) physical mixture (C), $PVA_{4\text{-}88}$-sorbitol (60:40)
529 cryomilled extrudate (D) and sorbitol (E) at 21 °C.

530

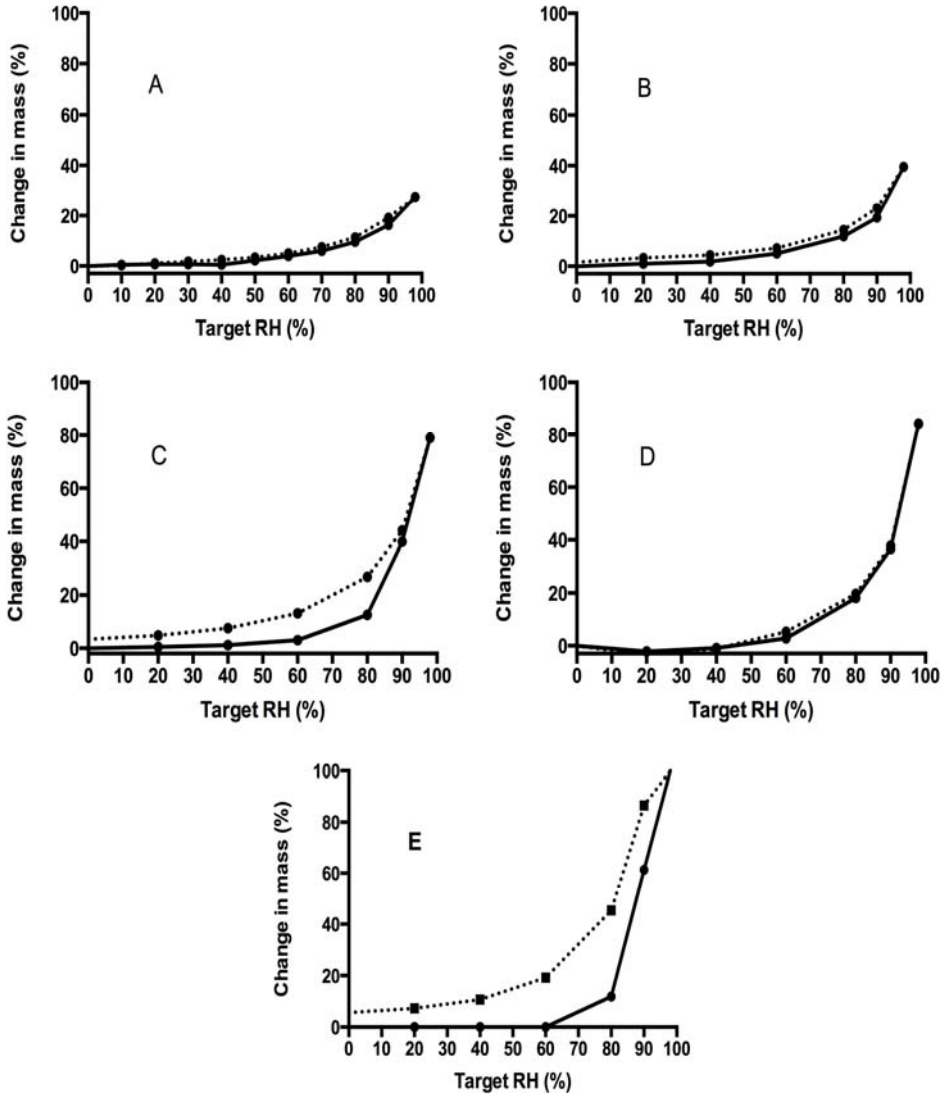

531

532

533

534

Figure 3: Tabletability of physical mixtures (PM) and hot-melt extruded (EX) samples formulated with PVA_{505} (A) or $PVA_{4\text{-}88}$ (B),, in combination with 0, 10 or 40% sorbitol (n=10).

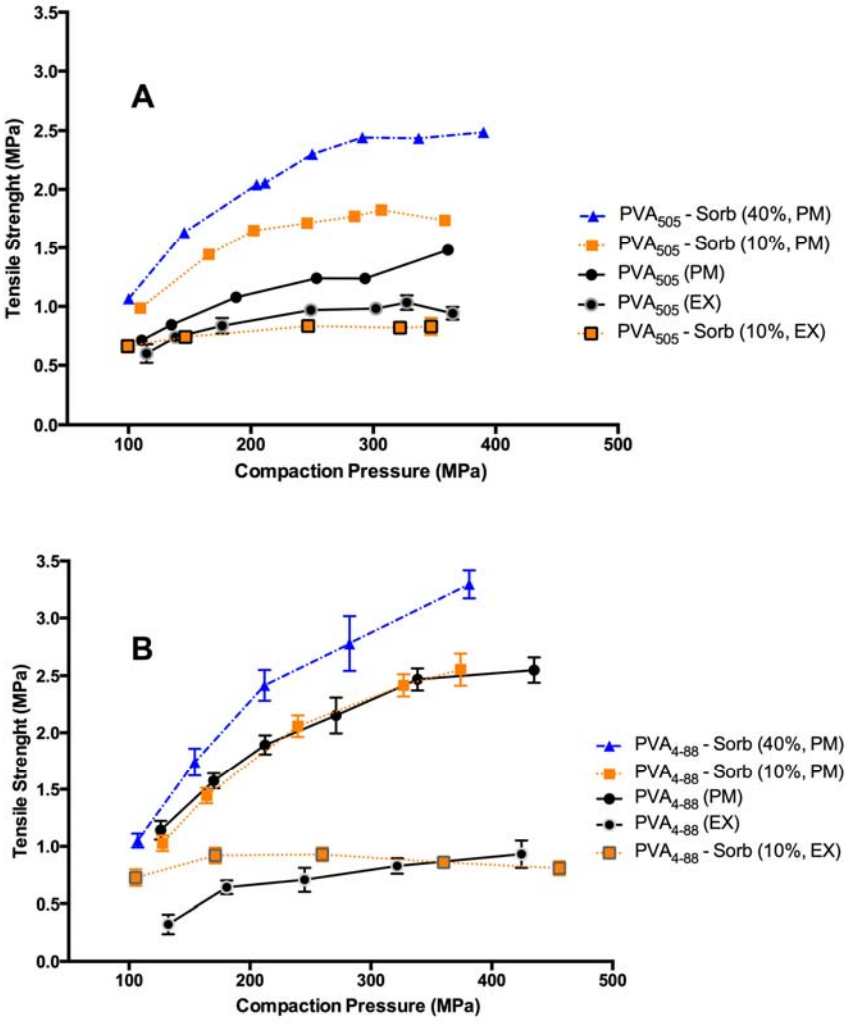

Figure 4: Compressibility of physical mixtures (PM) and hot-melt extruded (EX) samples formulated with PVA_{505} (A) and $PVA_{4\text{-}88}$ (B), in combination with 0, 10 or 40% sorbitol (n=10).

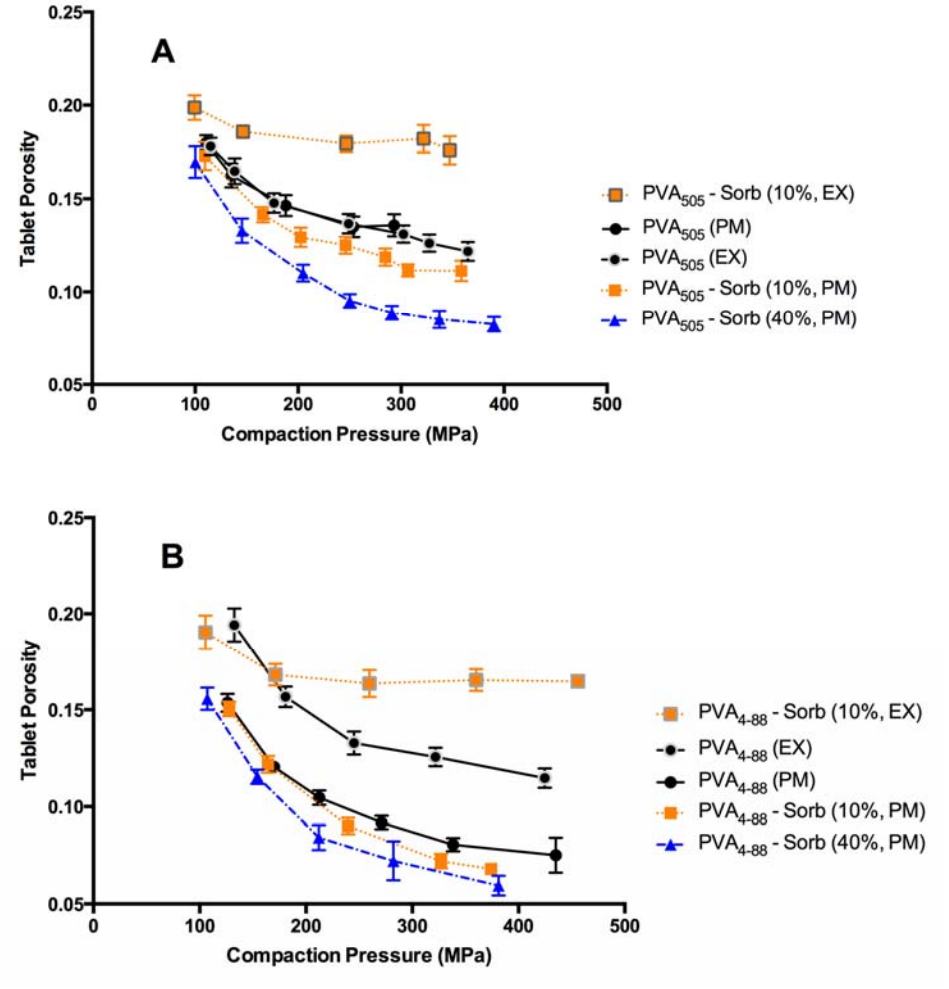

Figure 5: Compactibility of physical mixtures (PM) and hot-melt extruded (EX) samples formulated with PVA_{505} (A) or $PVA_{4\text{-}88}$ (B), in combination with 0, 10 or 40% sorbitol (n=10).

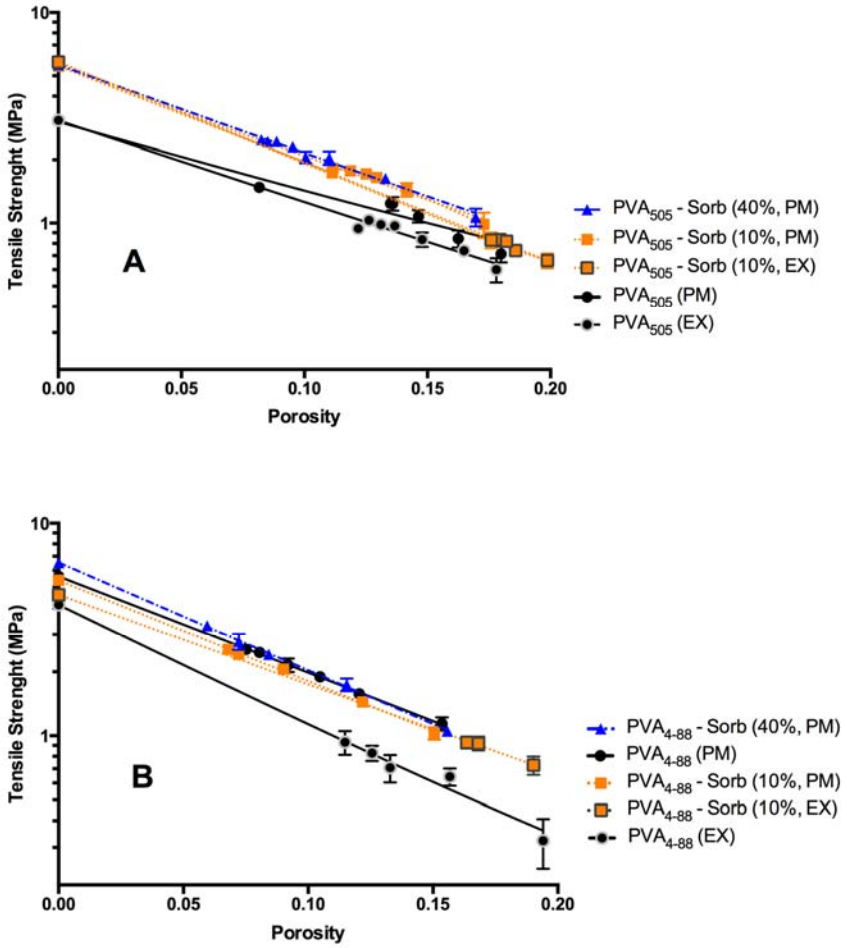

Figure 6: IAR-ratio of physical mixtures (PM) and hot-melt extruded samples (EX) at various compaction pressures for formulations containing PVA and sorbitol (n=10).

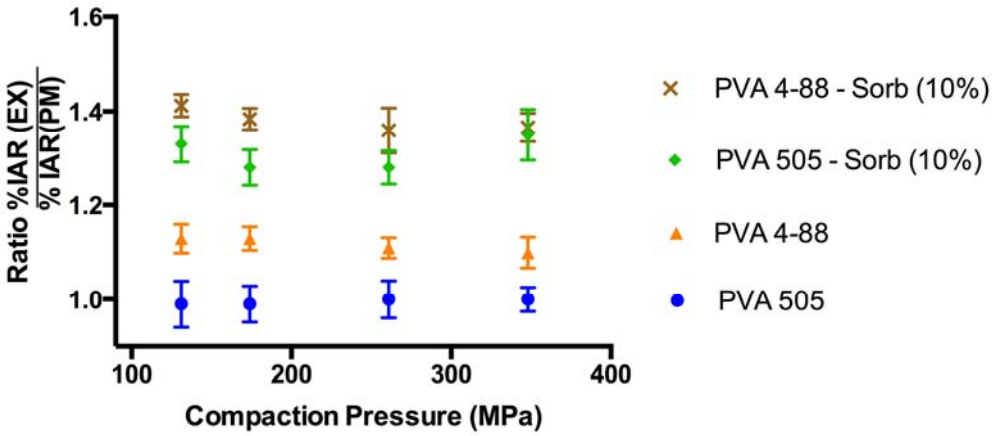

Table 1: Thermal properties of unplasticized and plasticized (containing 40% sorbitol) PVA after extrusion, cryo-milling and tableting using a heating rate of 10°C/min. The significance of the results was determined with ANOVA. Means of T_g (^{a,b}) or T_m (^{c,d}) in the same column with different superscripts are different at the 0.05 level of significance (Tukey) (n = 3).

Table 2: Solid-state ^{1}H-wideline NMR relaxation decay times (T_{1H}) and fractions (I_O) of $PVA_{4\text{-}88}$, sorbitol, physical mixtures and extrudates containing 40% and 10% sorbitol

Table 3: Mean particle size distribution of physical mixtures (PM) and cryo-milled extrudates (EX) of PVA/sorbitol formulations, measured via dry laser diffraction (n=3).

Table 1: Thermal properties of unplasticized and plasticized (containing 40% sorbitol) PVA after extrusion, cryo-milling and tableting using a heating rate of 10°C/min. The significance of the results was determined with ANOVA. Means of T_g (^{a,b}) or T_m (^{c,d}) in the same column with different superscripts are different at the 0.05 level of significance (Tukey) (n = 3).

				505 (72-75%)	**4-88** (88%)
UNPLASTICIZED (0% sorbitol)	1st heating		**T_g (°C)**	44.9 ±2.1	48.1 ±3.5
			$T_{m\ (ons.)}$ (°C)	155.0 ±1.4	164.1 ±1.6
	2nd heating		**T_g (°C)**	62.0 ±0.7	67.1 ±1.0
			$T_{m\ (ons.)}$ (°C)	131.5 ±6.6	144.7 ±9.6
PLASTICIZED (40% sorbitol)	2nd heating	**EXTRUSION**	**T_g (°C)**	34.3 ±3.2^a	38.6 ±1.1^a
			$T_{m\ (ons.)}$ (°C)	117.7 ±2.4^c	133.1 ±4.7^c
		CRYOMILLING	**T_g (°C)**	30.5 ±2.5^a	37.9 ±3.4^a
			$T_{m\ (ons.)}$ (°C)	121.8 ±5.2^c	149.1 ±3.3^d
		TABLETING	**T_g (°C)**	31.6 ±1.5^a	38.2 ±5.0^a
			$T_{m\ (ons.)}$ (°C)	131.2 ±3.8^d	149.1 ±2.2^d

Table 2: Solid-state ^{1}H-wideline NMR relaxation decay times (T_{1H}) and fractions (I_O) of $PVA_{4\text{-}88}$, sorbitol, physical mixtures (PM) and extrudates (EX) containing 40% and 10% sorbitol

SAMPLE	T_{1H} (s)			
	T_{1H}^S	I_o^S (%)	T_{1H}^L	I_o^L (%)
$PVA_{4\text{-}88}$	6.3	100.0		
Sorbitol			26.3	100.0
$PVA_{4\text{-}88}$-Sorbitol (60:40) PM	6.0	63.4	25.4	36.6
$PVA_{4\text{-}88}$-Sorbitol (60:40) EX	3.5	88.0	15.7	12.0
$PVA_{4\text{-}88}$-Sorbitol (90:10) EX			14.2	100.0

681 **Table 3:** Mean particle size distribution of physical mixtures (PM) and cryo-milled extrudates (EX) of PVA/sorbitol
682 formulations, measured via dry laser diffraction (n=3).

683

		d_{10} (µm)	d_{50} (µm)	d_{90} (µm)
PVA_{505}	**PM**	47.6 ±5.96	204.3 ±4.74	404.1 ±32.98
	EX	68.8 ±0.07	187.6 ±0.69	359.1 ±6.39
$PVA_{4\text{-}88}$	**PM**	22.9 ±0.52	164.4 ±16.71	544.0 ±7.41
	EX	73.4 ±4.43	203.0 ±5.78	367.2 ±4.15

684